JOURNAL OF AEROSPACE COMPUTING, INFORMATION, AND COMMUNICATION
Vol. 1, September 2004

On-Line Processing of Pressure-Sensitive Paint Images

Wim Ruyten†* and Marvin Sellers†
Aerospace Testing Alliance, Arnold AFB, Tennessee 37389-6400

This paper documents a milestone that has been reached at the Arnold Engineering Development Center, namely to reduce data reduction times for both intensity-based and lifetime-based pressure-sensitive paint measurements from an eight-camera system sufficiently that one data point can be processed in full (in 5 to 10 s) while the next data point is being acquired. The paper describes the hardware, software, and data reduction strategies used, and it presents results for benchmark data from wind tunnel tests on scale models of an F-16C fighter jet and NASA's X-38 Crew Return Vehicle.

I. Introduction

PRESSURE-SENSITIVE paint (PSP) has established itself as an important test and evaluation tool for mapping pressure distributions on aerodynamic test articles, particularly in transonic wind tunnels.[1-7] Most commonly, the luminescence from the painted test article is captured using digital cameras. Thus, PSP is essentially an image-based technique. (The much less frequently used approach based on a scanned laser spot system is not considered here.) To achieve full coverage across the surface of the test article, multiple cameras are typically used. Data are then processed and presented to the test customer either in two-dimensional image format or as data that have been mapped to a three-dimensional grid of the test article. The latter format is preferred because it allows force and moment integrations to be performed, across either the whole surface or parts thereof.

Considerable computational resources are required to convert raw images into fully processed PSP data. In the past, days or weeks were required to perform this task. Over the years, analysis techniques have become more sophisticated and computers have become faster, making it possible, at present, to process data while a wind tunnel test is in progress. The purpose of this paper is to review the technology that has made this milestone possible at the Arnold Engineering Development Center (AEDC).

II. Theory

A. Paint Response

The theory behind PSP has been reviewed extensively elsewhere.[1,2] At the heart of PSP processing is the notion that the pressure, P, can be obtained from a ratio, R, of two signals, $S^{(1)}$ and $S^{(2)}$, by a calibration function, $P(R,T)$, where T is the temperature. Symbolically, this may be written as

$$R_{ij} = S_{ij}^{(1)} \Big/ S_{ij}^{(2)}, \tag{1}$$

and

$$P_{ij} = P(R_{ij}, T). \tag{2}$$

Presented as Paper 2003-3947 at the 21st Applied Aerodynamics Conference, Orlando, Florida, 23-26 June 2003; received 25 February 2004; revision received 25 June 2004, accepted for publication 6 July 2004.

* Engineer Specialist, AIAA Associate Fellow.
† Senior Engineer.

The subscripts *ij* indicate that the respective quantities may be thought of as pixel values in a digital image. The pressure from Eq. (2) is usually converted to a pressure coefficient according to the relation

$$c_{p,ij} = (P_{ij} - P_\infty)/Q, \tag{3}$$

where P_∞ and Q are the freestream static and dynamic pressures, respectively.

In intensity-based PSP, continuous illumination is used, and the signals $S^{(1)}$ and $S^{(2)}$ in Eq. (1) are the wind-off and wind-on signals, respectively, with ambient pressure providing the wind-off reference signal. In lifetime-based PSP, pulsed illumination is used. This allows both $S^{(1)}$ and $S^{(2)}$ to be obtained at the run condition, by integrating different parts of the fluorescence decay profile, namely, at different gate delays with respect to the excitation pulse train.

The calibration function *P(R,T)* is typically cast in the form of a polynomial with fixed coefficients.[3,8] Figure 1 shows an example of a set of calibration curves for the paint PtTFPP in FIB,[9] which is produced by Innovative Scientific Solutions, Inc. and is the current industry standard for large-scale PSP testing in the U.S. Ideally, the temperature, *T*, in Eq. (2) would be provided on a per-pixel basis. In practice, a single, average value is typically supplied.

More complex implementations of PSP are possible—for example, those based on the use of bilumiphore paints[10,11] or those based on multigate imaging.[12,13] In such alternate schemes, two signal ratios are defined, allowing either the determination of a temperature-corrected PSP measurement or a combined pressure and temperature measurement. In the following, it is assumed that only a single signal ratio is used for data processing.

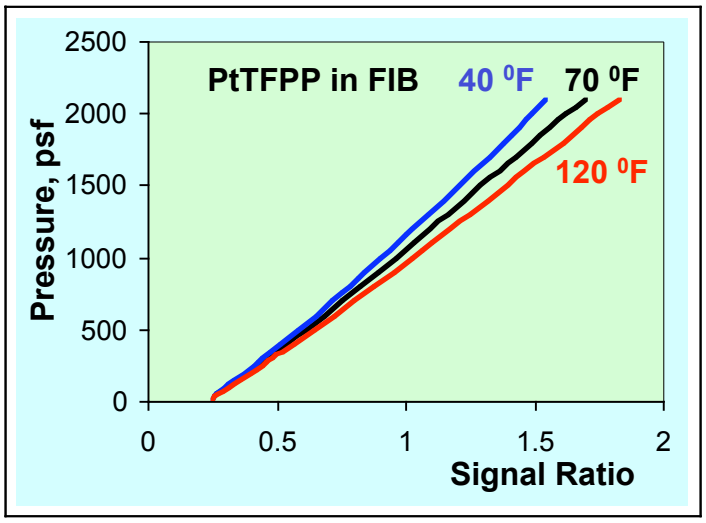

Fig. 1 Example of PSP calibration curves.

B. Image Mapping

To establish the mapping transformation between two-dimensional image coordinates and three-dimensional spatial coordinates on the surface of the test article, registration targets are applied to the test article. Let $\boldsymbol{X}_n$ denote the three-dimensional model coordinates of the target with index n, as determined by a coordinate measuring machine. The resulting image coordinates, (x_n, y_n), may be written symbolically as[14,15]

$$(x_n, y_n) = F(\mathbf{X}_n; \mathbf{p}_c^*, \mathbf{q}_c, \mathbf{a}_m, \mathbf{t}), \tag{4}$$

where the function $F(\ldots)$ represents a projective transform (see Fig. 2) that takes as input the three-dimensional model coordinates, $\boldsymbol{X}_n$, of the targets; the set of exterior parameters, $\mathbf{p}_c^*$, for camera *c* (representing the position and orientation of camera *c* with respect to the test facility); the set of interior parameters, $\mathbf{q}_c$, for the same camera (representing the effective focal length, optical center, and lens distortion parameters); a set of angles, $\mathbf{a}_m$, that describes the pitch and roll settings of the model-positioning system at a model attitude *m*; and a fixed set of model alignment parameters, **t**.

Before the function $F(\ldots)$ can be determined for a given image, the image coordinates, (x_n,y_n), of a sufficiently large set of targets must be obtained. This requires that the registration targets be located and identified in a set of images (see Fig. 3). To do this automatically and efficiently has been the single biggest challenge in achieving on-line processing of PSP data. Aspects of this task are described elsewhere,[16,17] and a detailed description may be found in Ref. 18. In short, the image locations of the visible registration targets are estimated based on the reported attitude angles of the wind-tunnel model, and a template-based correlation technique is used to find the targets with subpixel accuracy. (The ellipses in the insets in Fig. 3 indicate the outlines of the search templates, which are calculated based on the known physical size of the targets.)

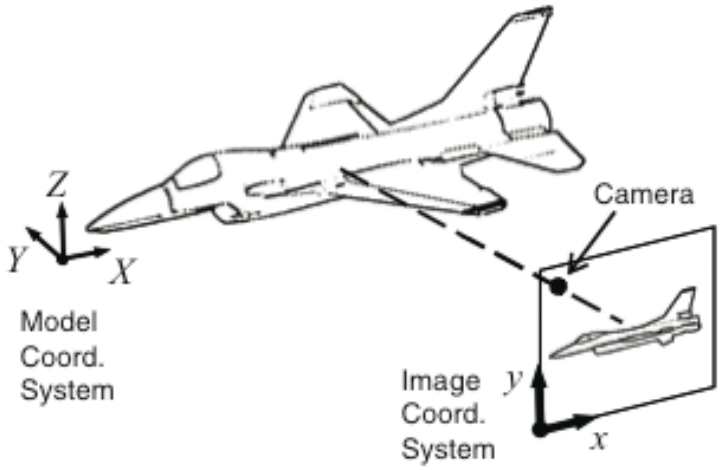

Fig. 2 Projection of three-dimensional model coordinates into a two-dimensional image.

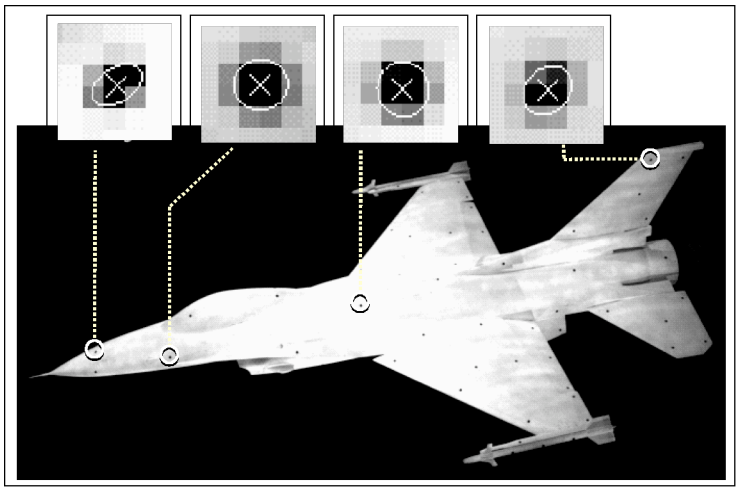

Fig. 3 Example of PSP image with registration targets.

Once the mapping function, F, is known, it may be used to map image pixels to the predefined three-dimensional grid of the test article. This typically involves the use of a z-buffer to preclude image data from being mapped to occluded parts of the three-dimensional surface grid.[18] So far, only multizone structured grids have been used as three-dimensional grids. The use of unstructured grids (which are often simpler to create) is under consideration and should require only straightforward (though extensive) changes to the data reduction software.

A related image registration problem in intensity-based PSP is that of aligning a wind-on image to a wind-off image. If the misalignment between the two images is not too severe, the image coordinates in the second image may be related to the image coordinates in the first image by a polynomial transformation that may be written symbolically in terms of a function G as: [19,20]

$$(x_n^{(2)}, y_n^{(2)}) = G(x_n^{(1)}, y_n^{(1)}). \tag{5}$$

C. Self-Illumination (SI) Correction

When emitted light from a low-pressure region on the surface of the test article (i.e., a region with relatively high signal) is emitted toward a high-pressure region (i.e., a region with relatively low signal) and is reflected toward the camera, the increased signal caused by the reflection process tends to lower the measured pressure. To a lesser extent, measured pressures in low-pressure regions are affected as well. It is possible to correct for these effects by approximating the painted surface as a diffuse reflector. The net emitted signal, S'_k, at a point k on the three-dimensional grid may then be obtained from the measured signals, S_l, at other points l according to

$$S'_k = S_k - R_{\text{diff}} \sum_l A_{kl} S_l , \tag{6}$$

where R_{diff} is the reflectivity of the paint, A_{kl} is an influence coefficient that depends only on the geometry of the test article, and the summation is over that part of the surface with nonzero influence coefficients.[21] Higher-order corrections, based on the use a bidirectional reflection distribution function, are also possible.[22]

The SI correction from Eq. (6) needs to be performed separately on both of the signal terms in Eq.(1). This implies that the image data must be mapped to the three-dimensional grid before a signal ratio is calculated. In this regard, SI corrections require a deviation from the conventional data-processing sequence, in which data from each camera, separately, are processed to a pressure distribution on the three-dimensional grid.

The A-matrix from Eq. (6) can be precalculated, allowing the SI correction to be performed efficiently. Moreover, because the reflected light is, by assumption, diffusely distributed, the SI correction needs to be calculated explicitly only for a fraction of the grid points (10%, typically). The SI correction at the remaining points can then be obtained by interpolation.

III. Processing Schemes

More than 70 macro commands are built into the actual software. The most important of these can be grouped into the following eight processing steps.

DEFINE: Locate the required input data files based on the to-be-processed run and sequence numbers, and generate the names of the resulting output files.

LOAD: Load data files into memory and perform one or more of the following: Subtract a black image (an "image" collected with the lens covered); divide by a flat-field image (an "image" collected without a lens on the camera, with the CCD array exposed to a uniform light field); scale the image by an exposure time or by the number of pulses over which the integration was performed; and/or apply a threshold value below which image data are considered to be indistinguishable from the background. Flat-field corrections are particularly important for intensity-based PSP measurements in low-speed flow (when small model shifts between wind-off and wind-on images can have a significant effect), but are typically not used for transonic testing at AEDC.

REGISTER: Find (to subpixel precision) and identify all of the visible registration targets in the image and determine the resulting mapping transformation between three-dimensional model coordinates and two-dimensional image coordinates, as expressed by Eq. (4). These mapping transformations are based on the use of photogrammetry, as described in Refs. 14 and 15. Two tasks typically performed along with image registration are the calculation of the location of visible pressure taps (for use with in-situ calibrations, see below) and removal of registration targets and other artifacts by patch-interpolation.

ALIGN: Given the image coordinates of registration targets in a set of wind-off and wind-on images, determine the coefficients of the image alignment transformation from Eq. (5) and apply the transformation to align the two images. This alignment is only needed for intensity-based PSP measurements, to compensate for the shift in model position that occurs as a result of sting deflection.

CONVERT: Calculate the ratio from Eq. (1), either between two images or between two sets of data on the same three-dimensional grid. Set the result to "undefined" for points that do not have a valid value in both sets; then convert the ratios to pressure using Eq. (2), or to a pressure coefficient using Eq. (3). If pressure readings from pressure taps on the model are available, these may be used to adjust Eq. (3) to obtain optimum agreement between

the PSP-derived values in the vicinities of the taps and the tap values themselves. (This process is known as in-situ calibration.)

MAP: On the basis of Eq. (4), map two-dimensional image data to the predefined three-dimensional grid of the test article. In doing so, mapped values at the grid points are assigned based on weighted values from the corresponding image pixels. To prevent mapping to occluded parts of the three-dimensional grid, a z-buffer algorithm is used to determine visibility. If the same grid point is mapped by two or more cameras, the camera with the view that is most nearly normal to the surface is used.

SI-CORRECT: Perform the self-illumination correction from Eq. (6).

SAVE: Save intermediate or final data to the hard disk in three-dimensional grid format. In addition to the pressure or pressure coefficient at every grid point, the saved file contains, for each grid point, the camera number from which the mapped point was obtained and the cosine of the viewing angle for that camera, for use with mapping.

Figure 4 shows two processing sequences based on the eight processing steps above. Both sequences lead from two sets of raw image data ("1" and "2" in Fig. 4) to pressure coefficients on a three-dimensional grid (denoted as set "3" in Fig. 4). The same steps are followed for both intensity-based and lifetime-based PSP, though the alignment step is typically not required for lifetime-based PSP. Likewise, a single registration step typically suffices for both images in lifetime-based PSP processing. The primary difference between the two sequences in Fig. 4 is the point at which two-dimensional image data are mapped to the three-dimensional grid. In the second sequence, this mapping is performed prior to the conversion to pressure, so that the SI correction from Eq. (6) can be performed. Alignment of the two sets of raw images is not needed in this case.

Dashed lines are used in Fig. 4 to indicate which macros have to be performed for each of the eight cameras individually. This grouping of macros has implications for parallel processing, which is discussed in Sec. V.C.

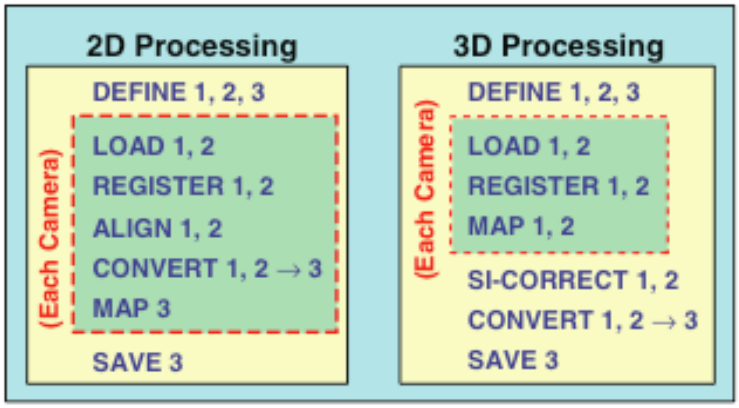

Fig. 4 Basic processing sequences.

IV. Benchmarks

Two data sets have been selected to serve as benchmarks for timing studies (see Table 1). These are small subsets from actual PSP tests on scale models of an F-16C fighter jet[3] and NASA's X-38 Crew Return Vehicle (see Fig. 5). Both tests were conducted in the 16-ft Transonic Wind Tunnel (16T) at AEDC, with eight cameras mounted in the test section, as shown in Fig. 6. (Only six cameras were used for the actual data reduction on the X-38.) In both tests, FIB-based paints were used (see Table 1) as the basis for an intensity-based measurement, while excitation of the PtTFPP fluorophore was accomplished with xenon arc lamps, filtered between 350 and 550 nm.

In both benchmarks, four images are used per camera per data point (wind off and wind on, each with associated black images). Image sizes are 1024x1024 pixels, with 16-bit resolution per pixel. Both benchmarks contain four model attitudes, taken from an alpha sweep. The three-dimensional geometry files for both tests are multizone, structured, PLOT3D grids with over 300,000 grid points each. In both cases, self-illumination corrections were performed at about 1/10 of this resolution, with on the order of 30,000 cells per calculation. Further details are given in Table 1. Figure 7 shows an example of the effect of the SI correction on the X-38.

Table 1 Benchmark Data Sets

	F-16C	X-38
Number of Data Points	4 (α = 0, 8, 18, 26 deg)	4 (α = 4, 8, 16, 20 deg)
Mach Number	0.8	0.6
Number of Cameras	8	6
Paint	PtTFPP in FIB7	PtTFPP in UniFIB
Images per Camera per Point	4	4
Image Size	1024×1024×16 bit	1024×1024×16 bit
Number of Registration Targets	102	36
Number of Pressure Taps	400	118
Number of Zones per Grid	379	264
Number of Points on 3D Grid	344,269	311,726
Number of Elements in A-Matrix	29,172	31,344
Size of A-Matrix File	230 MBytes	129 MBytes

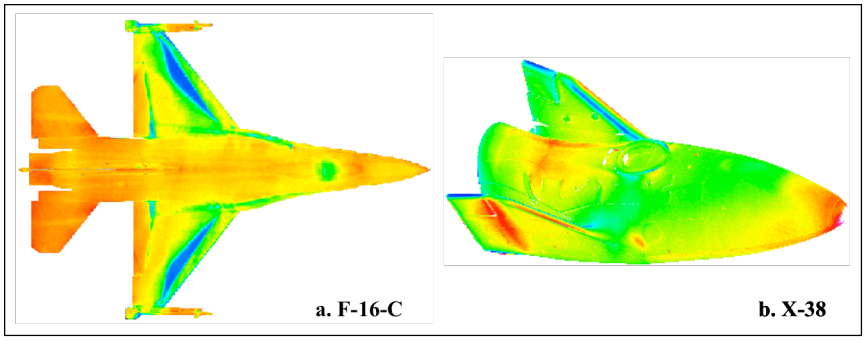

Fig. 5 Examples of processed data for the two benchmark cases.

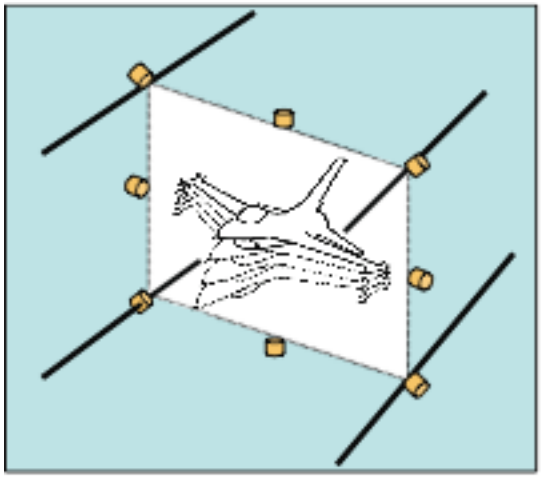

Fig. 6 Schematic of wind tunnel setup with positions of the eight cameras shown.

V. Software and Hardware

A. Software

Since 1998, PSP data processing at AEDC has been accomplished with "Green Boot," a program that was developed in the mid 1990s by McDonnell Douglas Aerospace (MDA) and NASA Ames. Since the program was

acquired by AEDC, NASA Ames and AEDC have continued development of a Government version of the code, while Boeing (upon acquiring MDA) has continued development of a proprietary version. The Government version of the code (currently, Version Gb.2.17a) consists of about 92,000 lines of code, programmed 88 percent in C and 12 percent in Fortran. The program has an extensive graphical user interface (GUI) but also supports script-based processing. The program runs on either SGI Irix or Linux platforms. The program structure is essentially sequential, though modifications have been made to support parallel processing, as described in Sec. V.C.

Table 2 lists the principal support files for the Green Boot program. The SQL database file keeps track of all raw and processed images associated with a particular test, as well as associated parameters such as tunnel conditions and mapping coefficients. The targets file contains model coordinates, normal vectors, and (when applicable) diameters of each of the targets and pressure taps, as well as other points ("fiducials") that need to be located in the image but that are not used for image registration. The camera file stores parameters that are required to accomplish automatic image registration. The setup file contains various program settings and maintains a list of most-recent commands. The Wind Tunnel Data (WTD) files report tunnel conditions and aerodynamic coefficients, as well as pressure readings from pressure taps, if any, to be used for in-situ calibrations. The three-dimensional grid file defines the geometry of the test article. The component file defines groupings of zones for load calculations on parts of the model (e.g., left upper wing, left lower wing, fuselage, etc.). The A-matrix file contains the precalculated SI coefficients from Eq. (6). Macro files define processing sequences such as those in Fig. 4. The log file and diagnostics files maintain a record of submitted inputs and outputs generated by the program.

Table 2 indicates whether the files are used for input, output, or both, and whether the files are used as part of the manual pretest calibration process, which has to be completed before fully automated processing can be accomplished in run mode.

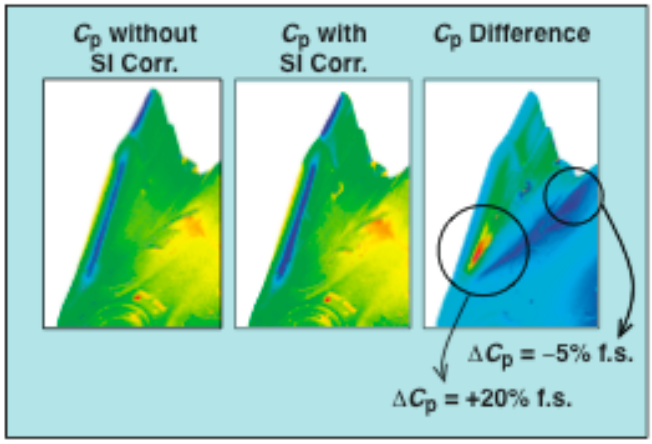

Fig. 7 Illustration of effect of self-illumination correction on X-38 tail section.

Table 2 Support Files for Data Processing

	Input	Output	Calibration
SQL Database File	✓	✓	
Targets File	✓		
Camera File	✓		✓
Setup File	✓	✓	✓
WTD Files	✓		
3D Grid File	✓		
Component File	✓		
A-Matrix File	✓		
Macro Files	✓		
Log File		✓	
Diagnostics Files		✓	

B. Hardware

The Green Boot code has been run on a variety of Silicon Graphics workstations, from the now-obsolete Indigo 2 and O2, through the Origin 2000, the Octane, and Octane 2, with processors ranging from an IP22, R4400 for the Indigo 2 to a dual IP 30, R14000 for the Octane 2, and at processing speeds ranging from 195 MHz for the Indigo 2 to 600 MHz for the Octane 2.

Until recently, all PSP data acquisition (along with a large part of the data processing) was performed on an SGI Origin 2000, equipped with 1.3 GB of memory and with eight IP27, R10000 processors running at a (now slow) speed of 195 MHz.

Most recently, the Green Boot code has been transitioned to a Linux cluster. This system is configured to allow simultaneous data acquisition and data processing. It consists of a set of front end, dual P4, Xeon processors running at 2.4 GHz and eight dual-processor slaves (also P4 Xeons), each running at 2.2 GHz. Communication between the master and the slaves is through an HP switch with a 1-Gbit Ethernet connection to the front end and 100-Mbit connections to each of the nodes. The front end has 2 GB of memory, while the nodes have 1 GB each. Both the master and the slaves run Linux Red Hat 7.3 (kernel version 2.4.18-17.7.xsmp) as the operating system.

C. Implementation

Various configurations of the software have been employed, ranging from purely sequential processing (i.e., one camera at a time) to parallel processing as shown in Fig. 8. The implementation shown in Fig. 8 is the latest and fastest, especially if a separate processor is available for each of the processes shown (i.e., one master process and up to eight slave processes).

The implementation from Fig. 8 applies to both processing sequences from Fig. 4. In each case, macros in the dashed boxes in Fig. 4 are performed in parallel for each camera individually. Upon completion, partially processed data from all cameras are combined and processed to final data on the three-dimensional grid. Communication between the master process and the slaves is accomplished by using the UNIX concepts of forks and pipes on an SGI architecture, and by a TCP/IP-based scheme on the Linux cluster. These schemes are discussed in detail in Ref. 23.

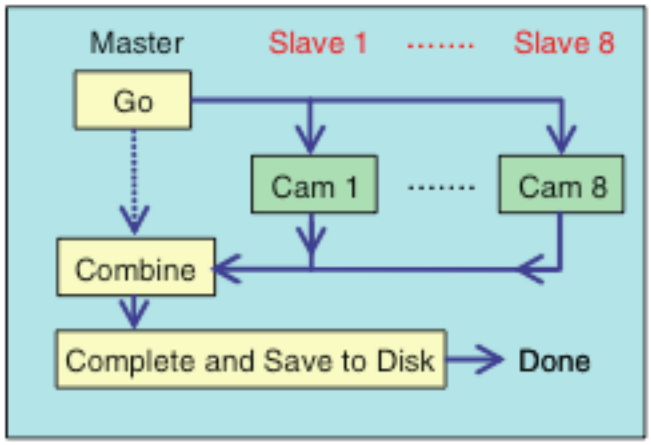

Fig. 8 Parallel processing implementation for the processing schemes from Fig. 4.

VI. Timing Results

Benchmark results for the data from Sec. IV are presented in Tables 3 and 4. In these tables, the designations "2D" and "3D" refer to the processing schemes from Fig. 4. In each case, the highest possible optimization settings were used at compile time, i.e., the "-O3 –r12000" flags on the SGI machines and the "-O" flag on the Linux machines.

Table 3 reports average processing times per processing step for the X-38 data set on the SGI Indigo 2, when only a single processor was used. It is seen that the most time-consuming processing steps are image registration and mapping data to the three-dimensional grid. Mapping times in the three-dimensional case are twice those in the two-dimensional case, which is consistent with the fact that twice as many images have to be mapped (i.e., wind-off and wind-on intensities, as opposed to pressure values).

Table 3 Cumulative single-processor times (in seconds) for X-38 data on SGI Octane 2

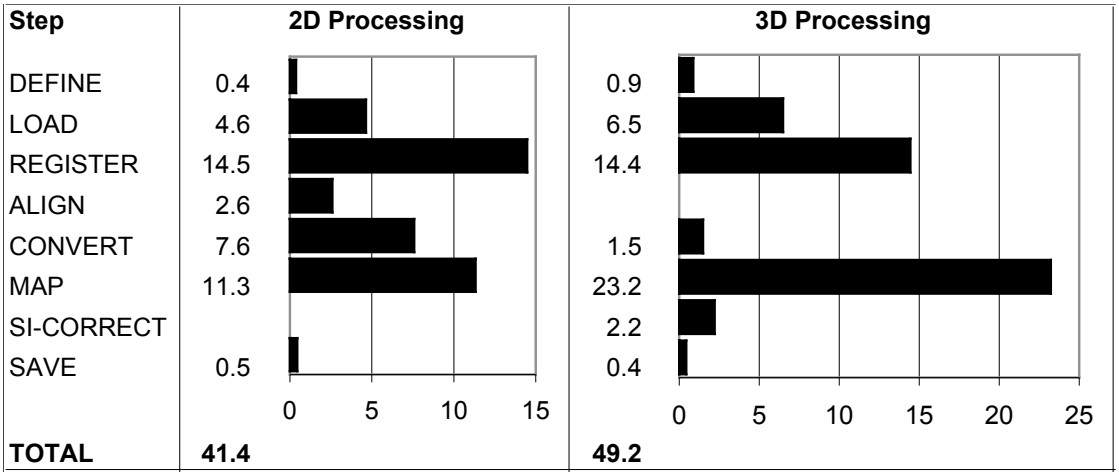

Table 4 lists total processing times per model attitude for both the F-16C and X-38 data sets. Times are grouped by machine, by processing type (two-dimensional vs three-dimensional—see Fig. 4), and by sequential ("seq") vs parallel ("par") processing. In the sequential case, only one processor is used per machine. This results in longer times for the F-16C data compared to the X-38, because of the use of eight cameras versus six, and because of the use of 102 registration targets for the F-16C vs 36 targets for the X-38. In the parallel case, either eight, two, or nine processors are used, as indicated by machine type. Times for the F-16C and X-38 are closer in this case, though the F-16C still requires more processing as a result of the larger number of targets. Most importantly, parallel processing times on the fastest machine (the Linux cluster) are well below 15 s per data point. This (15 s) was the target for achieving on-line processing, in the sense that one data point can be processed in full while the next data point is being acquired.

Table 4 Processing times per model attitude in seconds

	SGI Origin 2000 (8 Proc, 195 MHz)		**SGI Octane 2 (2 Proc, 600 MHz)**		**Linux Cluster (9 Dual Proc, 2.2 GHz)**	
	F-16C	**X-38**	**F-16C**	**X-38**	**F-16C**	**X-38**
2D, Seq	150	103	60	39	32	22
3D, Seq	193	121	74	48	41	28
2D, Par	27	22	30	22	7	6
3D, Par	41	31	38	28	10	8

VII. Concluding Remarks

By implementing parallel processing of PSP image data on a Linux cluster, a significant milestone has been achieved, namely the ability to reduce processing times sufficiently that one data point can be processed in full while the next data point is being acquired.

The processing schemes employed can easily be extended to more general PSP measurements, for example, those that would employ a third (and possibly a fourth) gate for simultaneous measurement of pressure and temperature,[10,12,13] or for a temperature-corrected PSP measurement.

Further reductions in data-processing times (with processing times moving below one second per data point) are probably not required for the study of steady-state flows. However, it is conceivable that further speed increases might become desirable for the study of unsteady flow phenomena such as buffet, flutter, limit-cycle oscillations, and other dynamic pressure phenomena. Such further improvements in data-processing times would probably call for both hardware and software improvements beyond those described here, or would use two-tier processing, with approximate data being generated in near-real time. More accurate processing would then be performed after the completion of the wind tunnel test.

Finally, the ability to perform PSP measurements in near real time could benefit the recent emergence of rapid model fabrication technologies for next-generation vehicles. That is, small, uninstrumented models might not only be manufactured from CAD models in less than one day, but tested in the same short timeframe as well.

Acknowledgments

The authors wish to thank Daryl Sinclair, Keith Anspach, J. Whitney Hebner, Bill Sisson, Ron Eads, Doyle Young, and Dr. James Bell for assistance and helpful discussions. Insights from two referees are also acknowledged. This work was supported, in part, by the Air Force Office of Scientific Research under the Test and Evaluation program, managed by Dr. Neil Glassman.

References

[1]Bell, J. H., Schairer, E. T., Hand, L. A., and Mehta, R. D., "Surface Pressure Measurements Using Luminescent Coatings," *Annual Review of Fluid Mechanics*, Vol. 33, 2001, pp. 155-206.

[2]Liu, T., Campbell, B. T., Burns, S. P., and Sullivan, J. P., "Temperature- and Pressure-Sensitive Paints in Aerodynamics," *Applied Mechanics Reviews*, Vol. 50, 1997, pp. 227-246.

[3]Sellers, M. E., "Application of Pressure Sensitive Paint for Determining Aerodynamic Loads on a Scale Model of the F-16C," AIAA Paper 2000-2528, June 2000.

[4]Baker, W. M., "Recent Experiences with Pressure-Sensitive Paint Testing," AIAA Paper 2001-0135, Jan. 2001.

[5]Bencic, T. J., "Calibration of Detection Angle for Full Field Pressure-Sensitive Paint Measurements," AIAA Paper 2001-0307, Jan. 2001.

[6]Engler, R. H., Klein, C., and Trinks, O., "Pressure Sensitive Paint Systems for Pressure Distributions Measurements in Wind Tunnels and Turbomachines," *Measurement Science and Technology*, Vol. 11, 2000, pp. 1077-1085.

[7]Bell, J. H., "Accuracy Limitations of Lifetime-Based Pressure-Sensitive Paint (PSP) Measurements," *Proceedings of the 19th International Congress on Instrumentation in Aerospace Simulation Facilities*, Aug. 2001, pp. 11-16.

[8]Bencic, T. J., "Temperature Correction for Pressure-Sensitive Paint," *NASA Tech Briefs*, Jan. 2000, pp. 50-51.

[9]Puklin, E., Carlson, B., Gouin, S., Costin, C., Green, E., Ponomarev, S., Tanji, H., and Gouterman, M., "Ideality of Pressure-Sensitive Paint. I. Platinum Petra (Pentafluorophenyl) Porphine in Fluoroacrylic Polymer," *Journal of Applied Polymer Science*, Vol. 77, 2000, pp. 2795-2804. (See also following three articles in same issue, by Gouin and Gouterman.)

[10]Hradil, J., Davis, C., Mongey, K., McDonagh, C., and MacCraith, B. D., "Temperature-Corrected Pressure-Sensitive Paint Measurements Using a Single Camera and a Dual-Lifetime Approach," *Measurement Science and Technology*, Vol. 13, 2002, pp. 1552-1557.

[11]Mitsuo, K., Asai, K., Hayasaka, M., and Kameda, M., "Temperature Correction of PSP Measurement Using Dual-Luminophor Coating," *Journal of Visualization*, Vol. 6, No. 3, 2003, pp. 213-223.

[12]Mitsuo, K., Egami, Y., Suzuki, H., Mizushima, H., and Asai, K., "Development of Lifetime Imaging System for Pressure-Sensitive Paint," AIAA Paper 2002-2909, June 2002.

[13]Watkins, A. N., Jordan, J. D., Leighty, B. D., Ingram, J. L., and Oglesby, D. M., "Development of Next Generation Lifetime PSP Imaging System," *Proceedings of the 20th International Congress on Instrumentation in Aerospace Simulation Facilities*, Aug. 2003, pp. 372-377.

[14]Liu, T., Cattafesta, L. N., III, Radeztsky, R. H., and Burner, A. W., "Photogrammetry Applied to Wind-Tunnel Testing," *AIAA Journal*, Vol. 38, 2000, pp. 964-971.

[15]Ruyten, W., "More Photogrammetry for Wind-Tunnel Testing," *AIAA Journal*, Vol. 40, 2002, pp. 1277-1283.

[16]Ruyten, W., "Automatic Registration of Luminescent Paint Images," *Proceedings of the 45th International Instrumentation Symposium*, 2-6 May 1999, pp. 279-288.

[17]Ruyten, W., "Subpixel Localization of Synthetic References in Digital Images by use of an Augmented Template," *Optical Engineering*, Vol. 41, No. 3, 2002, pp. 601-607.

[18]Ruyten, W., "Automatic Image Registration for Optical Techniques in Aerodynamic Test Facilities," AIAA Paper 2004-2400, June 2004.

[19]Bell, J. H., and McLachlan, B. G., "Image Registration for Luminescent Paint Sensors," AIAA Paper 93-0178, Jan. 1993.

[20]Bell, J. H., and McLachlan, B. G., "Image Registration for Pressure-Sensitive Paint Applications," *Experiments in Fluids*, Vol. 22, No. 1, 1996, pp. 78-86.

[21]Ruyten, W., and Fisher, C. J., "Effects of Reflected Light in Luminescent Paint Measurements," *AIAA Journal*, Vol. 39, No. 8, 2001, pp. 1587-1592.

[22]Ruyten, W., "Reconstruction of the Net Emission Distribution from the Total Radiance Distribution on a Reflecting Surface," *Journal of the Optical Society of America A*, Vol. 18, No. 1, Jan. 2001, pp. 216-223.

[23]Ruyten, W., and Sisson, W. E., "Message Passing for Parallel Processing of Pressure-Sensitive Paint Images," *Proceedings of the HPCMPO Users Group Conference*, 7-11 June 2004.